Journal of Power Sources, *33* (1991) 165–185

Pure lead and the tin effect in deep-cycling lead/acid battery applications

Robert F. Nelson* and **David M. Wisdom**
Gates Energy Products, Inc., Sealed-Lead Division, Warrensburg, MO (U.S.A.)

Abstract

The use of lead–calcium or pure lead grids in valve-regulated lead/acid (VRLA) batteries has been generally satisfactory, but one drawback of these materials is the unpredictable build-up of a passivation layer on the surface of the positive grid. In deep-cycling applications, this passivation layer can result in a rapid loss of discharge capacity that is reversible with proper treatment. This phenomenon is reminiscent of the 'memory effect' in nickel/cadmium cells and although it is reversible its unpredictability renders products not entirely suitable for deep-cycling applications. The use of small amounts of tin, alloyed into the positive grid or as a surface coating, has been promoted as a cure for this shortcoming, and to a large extent is effective. This paper presents a careful review of the 'tin effect' and provides information on how best to take advantage of minimal tin levels so that optimal cycling performance is realized. For example, it is noted that the nominal grid tin content may be less important than the way in which the metal is distributed. In VRAL products designed for deep-cycling applications, incorporation of tin into or on the surface of the positive grid in the proper way is of substantial benefit, if not crucial.

Introduction

The advent of valve-regulated lead/acid (VRLA) technology mandated the use of non-antimonial grid compositions, such as lead–calcium or pure lead, to minimize gassing and resultant dry-out. In the negative plate, this causes no serious problems and either material works quite well. In the positive, however, the use of non-antimonial grids is known to give rise to a passivation layer at the grid/active-material interface. This layer, first noted in flooded lead/acid systems [1], may also create difficulties in VRLA batteries in deep-cycling applications, as well as in the ability to recover from deep discharges. The nature of this passivation layer has been studied in great detail and its composition has been identified as being a mixed $PbSO_4/PbO_x$ structure ($1 \leqslant x < 2$) [2–4]. The PbO_x species have been identified as tetragonal PbO (tet-Pbo) and/or α-PbO_2, with the actual insulating passivation layer being tet-PbO deposited directly on the grid surface. Later work delineated the role of temperature and electrolyte in the anodic corrosion process [5], but it remained for Rüetschi to quantitatively characterize the structure and

*Author to whom correspondence should be addressed. Present address: Portable Energy Products, Inc., 940 Disc Drive, Scotts Valley, CA 95066, U.S.A.

0378-7753/91/$3.50

chemical environment of the grid/active-material interfacial area [6], thus confirming a qualitative model developed previously by Pavlov and co-workers [7–11]. Later work by Bullock and co-workers established that this passivation film could occur in acid-starved cells that had self-discharged to low potentials [12] and on lead sheet when it is corroded at high anodic potentials of about 1.35 V versus Hg/Hg_2SO_4 and above [13]. In functional batteries, it has also been shown that this 'sulphate barrier layer' can cause rapid cycle failure in thin-plate lead/acid cells and it was proposed that H_3PO_4 addition would correct the problem [14–16].

Thus, it has been demonstrated that a passivation layer can be generated on open-circuit stand, as well as during both cycling and overcharge/float; it can result in diminished capacity at best and, upon overdischarging, in complete loss of rechargeability under normal circumstances. The literature contains a bewildering array of conditions for generation of the passivation film, its composition and the chemistry involved. For the purposes of this study, the following may constitute an admittedly simplified picture of what actually occurs in a functional positive plate (many of the previously reported investigations are on bare metal grids or sheet).

When a positive plate is formed, or overcharged, an anodic corrosion film will be generated. The composition of the film will vary with the applied potential, being primarily α-PbO_2 at high positive plate voltages [13] or $PbSO_4$ at lower potentials [6]. The $PbSO_4$ or PbO_2 film acts as a permselective membrane, blocking the transport of SO_4^{2-} or HSO_4^-, but allowing the free passage of H^+, OH^- or H_2O species, as shown in Fig. 1. Any sulphate present in the interior layer will deposit out as $PbSO_4$ or mixed basic sulphates. In the alkaline medium that results, tet-PbO can form through anodic dissolution of lead near a pH of 9.34 via the following

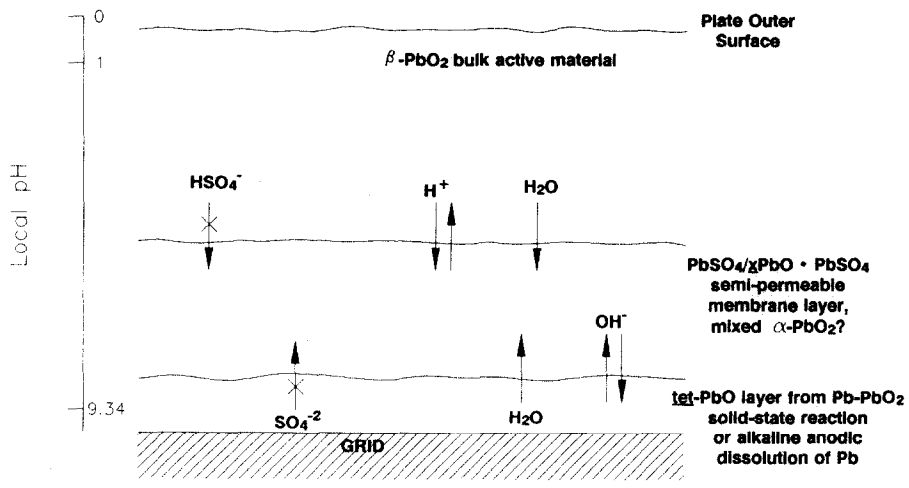

Fig. 1. Rüetschi model for lead/acid positive-plate structure for pure lead or lead–calcium grids.

reaction [6]:

$$5Pb + 7H_2O \rightleftharpoons 5PbO{\cdot}2H_2O + 10H^+ + 10e^- \quad (1)$$

At a somewhat lower pH of about 6.35 a mixed oxide/sulphate can form

$$2Pb + SO_4^{2-} + H_2O \rightleftharpoons PbO{\cdot}PbSO_4 + 2H^+ + 4e^- \quad (2)$$

and PbO can also be generated by the solid-state self-discharge process, shown most simply as

$$Pb + PbO_2 \rightleftharpoons 2PbO \quad (3)$$

In any event, the PbO formed at the grid interface is stabilized by the neutral or alkaline medium and acts as an electrical insulator toward current flow (actually, tet-PbO is a semiconductor). On overcharge, the tet-PbO thickness is reportedly about 4 μm and stays near that value due to a steady-state dissolution/deposition process that eats into the lead grid and presumably increases the size of the α-PbO_2 layer as it progresses, as shown in Fig. 2 [13]. The Bullock model is somewhat different from that of Rüetschi [6] in that the outer layer is an α-PbO_2 film that is more porous towards its outer border. At the PbO_2/PbO interface the tet-PbO is consumed and at the grid surface it is reformed, as shown in Fig. 2. Both processes are dependent upon oxygen diffusion rates and the constant 4 μm thickness is believed to be due to steady-state conditions governed by oxygen availability in the two reaction zones.

Clearly, this is a complicated topic, and it appears that the composition of the corrosion layer is greatly dependent upon the applied potential seen by the positive plate, as well as whether bare metal or a pasted plate is involved. This can be better understood by listing the various redox couples that can exist, in simplified form, along with their reported E_0' values versus Hg/Hg_2SO_4, all written as reduction potentials (Table 1).

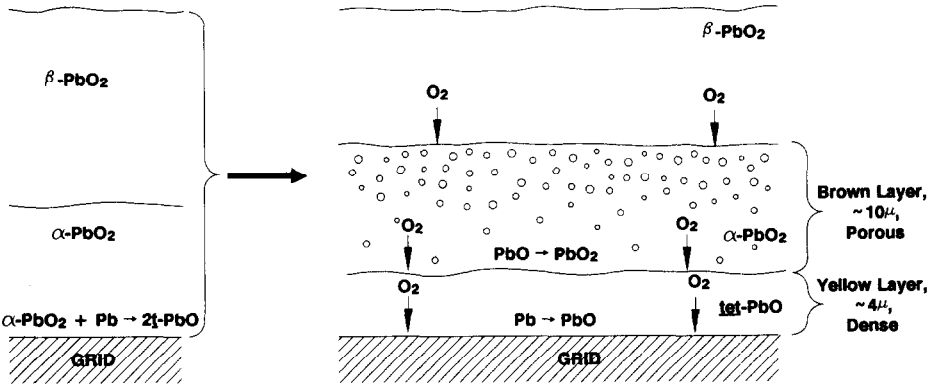

Fig. 2. Bullock model for lead corrosion layer generated by prolonged overcharge at $\geq$ 1.35 V vs. Hg/Hg_2SO_4/5.1 M H_2SO_4.

TABLE 1

Possible redox couples in corrosion layer

Electrode couple	Reference	Approximate E_0' value (V vs. $Hg/Hg_2SO_4/H_2SO_4$)
$PbSO_4/Pb$	6	−0.96
PbO/Pb	6	−0.38
α-$PbO_2/PbO{\cdot}PbSO_4$	6	~0.50
β-$PbO_2/PbSO_4$	6	1.12
α-$PbO_2/PbO/Pb$	13	$\geqslant$1.35

These potentials carry a number of implications for charge and discharge conditions. On charge, it is possible to generate tet-PbO at potentials only slightly above the $Pb/PbSO_4$ couple and if conditions are alkaline the PbO will be stabilized. On discharge, one would normally terminate the process just below the β-$PbO_2/PbSO_4$ potential (0.7 to 0.9 V), so if a tet-PbO layer were formed it would not be discharged. If one carries the positive plate voltage to 1.0 V negative the passivation layer should be consumed. Obviously, if the tet-PbO layer introduces a significant resistance into the potential measurements during discharge some of these comments may not apply; the influences of pH, diffusion potentials [6], activity effects and the like are also not considered.

It should be noted that this type of passivation layer has also been observed during processing of dry-charged battery plates after the conversion of the positive paste to PbO_2, the so-called 'thermopassivation' process [17, 18]. In principle, it can occur at any time after PbO_2 (for example, from red lead in the positive paste) is brought into contact with the lead grid and the temperature is near or above 100 °C, at which point the PbO_2/Pb solid-state reaction is promoted.

Generation of such a passivation layer in antimonial-grid products is apparently inhibited by the solubilities of the several antimony sulphate species formed [6]. The layer has also been moderated in lead–calcium batteries, perhaps fortuitously, by the incorporation of tin at levels of about 0.5 wt.% to improve fluidity during casting. The relationship between tin content and grid passivation has been known for some time [19, 20] and is well documented, but it is only recently that the 'tin effect' and grid passivation have been investigated in detail [21–24]. Tin is most easily incorporated (as an alloy) during casting but, because of its high cost, tin-rich surface layers of minimum thicknesses have been achieved by lamination [25, 26] or by electrodeposition [27–29] onto conventional positive-grid substrates. When directly alloyed into the grid, tin has been shown to be effective in providing recovery from deep discharge at a level as low as 0.3 wt.% [30], but in cycling applications as much as 2.5 wt.% tin has been reported necessary to eliminate early failures [31].

Tin incorporation has been shown, in general, to aid charge acceptance [30], and to reduce corrosion rates of bare metal grids [32] and top lead material [33]. More recently, it has been demonstrated that when tin/lead binary alloys are used in VRLA products considerable processing and performance advantages accrue [34]. The primary focus in the existing literature is the effect of the passivation layer upon recovery from deep discharge along with the relief afforded in processing by tin incorporation into the positive grid, but obviously there may also be effects in cycling and float applications. This paper presents data on the influence of the passivation layer on pure lead grids in deep-cycling service and how it can be overcome. It will also be shown that the nominal tin level may be of secondary importance to how the tin is incorporated. This latter point leads to some new findings on the mechanism of the 'tin effect'.

Experimental

All the pure lead cells and batteries used were standard production units. The lead–tin grid, flat-plate cells were prototype units nominally rated at 25 A h. Reference electrodes were standard $Hg/Hg_2SO_4/5.1\ M\ H_2SO_4$ hand-fabricated units. All electrical equipment used for charging and discharging cells was of the standard type commonly used in the battery industry.

Grid and plate samples were freeze-dried under vacuum to remove all acid after disassembly, where appropriate, under a nitrogen atmosphere. Once dried, samples were evacuated and impregnated with Hysol potting compound. After drying, the blocks were sectioned with a band saw and polished with standard grinding equipment.

Metallograhic photos were taken on a Leco model 300 metallograph with an Optomax image analysis system for thickness mapping.

SEDM/EDAX experiments were run on an ISI model SSI-40 unit with an IMIX system and an Omega light element X-ray detector.

Results

Batteries with pure lead or lead–calcium grids may experience unpredictable capacity losses in deep-cycling applications. In thin-plate cells, as noted, the presence of a passivation layer was tied to the rapid loss of capacity and the use of a phosphoric acid additive was proposed as a solution to the problem [14–16]. Experience with cells made with pure lead grids and quite thin plates (1 mm or less) has shown this not to be a viable solution.

In cells made with unsulphated, dense positive pastes it was felt that the capacity loss was due to the setting up of a fine plate porosity that resulted in the blocking of pores by lead sulphate as the positive plate discharged. Attempts to find a permanent solution have not been successful until recently. When tin was incorporated into the positive grid as an answer to poor

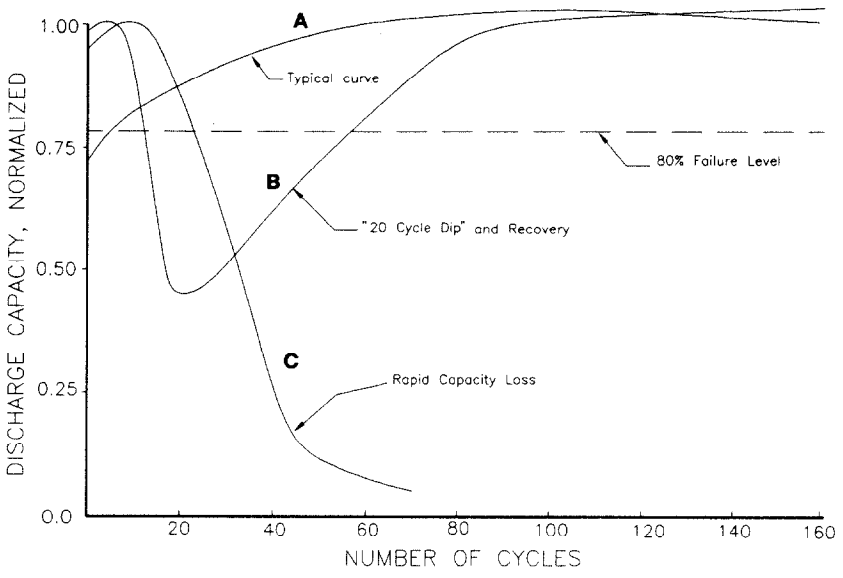

Fig. 3. Typical cycle/capacity plots for pure lead grid cells in deep-cycling applications.

deep-discharge recovery performance it was found that early deep-cycling behaviour was also markedly improved. In order to understand why this change took place, an in-depth comparison of pure lead and lead–tin cells was carried out.

Deep-cycling studies

Figure 3 contains several different cycle/capacity curves observed for pure lead grid cells on a $C/5$, one cycle per day regime. The 'typical' curve is the one most often seen, but occasionally cells will either experience a fairly rapid capacity loss or they will go through a 10–20 cycle 'dip' and then recover. In the case of the latter two types of cells or batteries, there is a rapid increase in impedance that will triple or quadruple the initial value within 10 to 15 cycles.

Rapid capacity loss has been found to be consistent within a particular batch of cells but not between batches. This behaviour is ameliorated, or eliminated, and cycle/capacity performance is more like curve A (Fig. 3) if the cells/batteries are either left to stand for an extended period (6 to 12 months) or are subjected to a heat soak. The latter is typically a simple oven treatment at 50 to 60 °C for 15 to 30 days, depending upon the severity of the condition.

Both of these processes involve time and temperature variations that would allow dissolution/recrystallization to occur within the passivation layer, which would slowly open up its structure and destroy the perm-selective membrane condition that maintains a high pH at the grid surface. Once acid and bisulphate penetrate to the grid surface area the tet-PbO will be

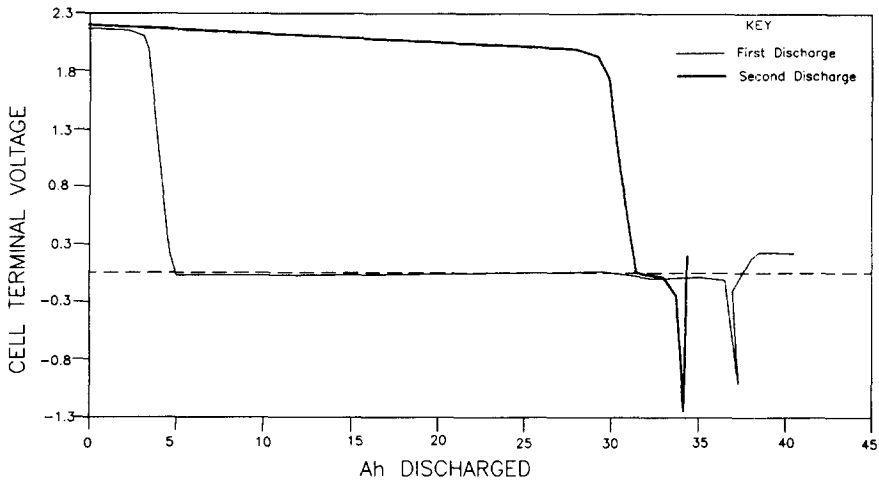

Fig. 4. 2 V/25 A h field return discharge data: two $C/50$ discharges to -1.0 V, cell voltage.

converted to neutral lead sulphate or mixed basic sulphates that, given time, will form larger and larger crystals via the digestion process. Obviously, if this process is allowed to take place for more extended times and/or at elevated temperatures 'hard sulphate' will form at the grid surface and the cell/battery will suffer from poor charge acceptance for a different reason [22, 23].

Interestingly, this capacity loss can also be reversed by carrying out one or more over-discharges to roughly -1.0 V/cell, as shown in Fig. 4. This is an extremely slow discharge at the $C/50$ rate, but similar results have been seen at discharge rates up to the $C/1$ level. The curves shown here are for a field return sample that only delivers less than 20% of its rated capacity to a normal 1.7 V cut-off on the first discharge. The cell voltage is driven all the way to zero volts and it stays there for most of the rest of the discharge. Figure 5 shows the corresponding discharge curves for each of the plates relative to a $Hg/Hg_2SO_4/5.1$ M H_2SO_4 reference electrode and it can be seen that the negative-plate voltage is reasonably constant until the end of the discharge and the bulk of the cell voltage 'dive' is due to the positive, which is driven deep into reversal. When the negative is exhausted the cell voltage then drops to the -1.0 V cut-off. Following recharge at a constant current of 1.5 A to 150% of the capacity removed, the second discharge exhibits a more normal behaviour. In fact, this cell, which had been in a field float application for 4 years, is indistinguishable from a new cell directly off formation in terms of discharge capacity and plate voltages.

This remarkable recovery of discharge capacity is apparently due to dissolution of the tet-$PbO/PbSO_4$ layer(s) at the grid surface as the positive is driven to high negative voltages. There is no 'typical' behavior for cells that have built up this passivation layer; discharge curves can vary from that shown in Fig. 4 to a double plateau, with the second one near or below the

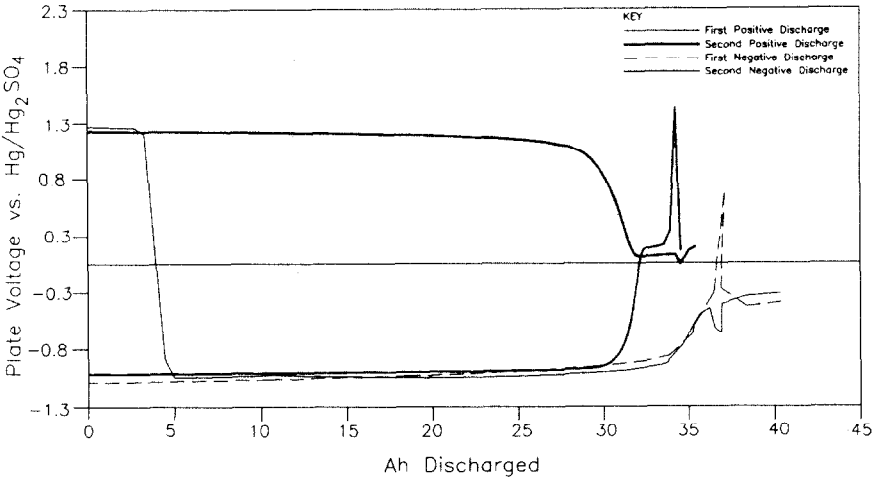

Fig. 5. 2 V/25 A h field return discharge data: $C/50$ discharges to -1.0 V, positive and negative plate voltages.

normal cut-off voltage. In studying many of these cells, it has been observed that, for optimal improvement, the positive must be driven to zero volts or negative and the number of amp-hours passed is proportional to the capacity gain in subsequent discharges. Throughout all the testing, it did not appear that the negative plates were involved in any way in this abnormal behaviour; failure and recovery depended almost entirely on the positive plate.

During discharges at the $C/1$ rate, it was noted that some of these 25 A h cells that had been returned from the field with low capacities became quite hot towards the end of the first discharge taken to -1.0 V. On subsequent discharges, the capacities were greatly improved and the temperatures stayed at moderate levels. In order to monitor temperature more closely, discharge tests were run at the $C/5$ rate, as shown in Fig. 6, and cell skin temperatures were recorded concurrently. The first discharge shows a double plateau with the second one being below the normal 1.7 V cut-off. Following the second plateau, the cell voltage drops to near zero volts and rides there until the negative electrode is completely discharged. The temperature begins to rise early in the discharge at the end of the first step. This continues as the cell goes through the second discharge step: the temperature peaks at about 31 °C above ambient (actual temperature of 54 °C) and then slowly drops until the discharge is completed. On the subsequent discharge, a normal single plateau is observed and there is little increase in temperature until near the end of the discharge when resistive effects due to electrolyte depletion and secondary chemical reactions may cause the cell to heat up somewhat. Alternatively, the moderate rise may be due to a residual passivation layer.

The above is a striking experiment with significant implications in field applications. Note that the temperature build-up during both discharges

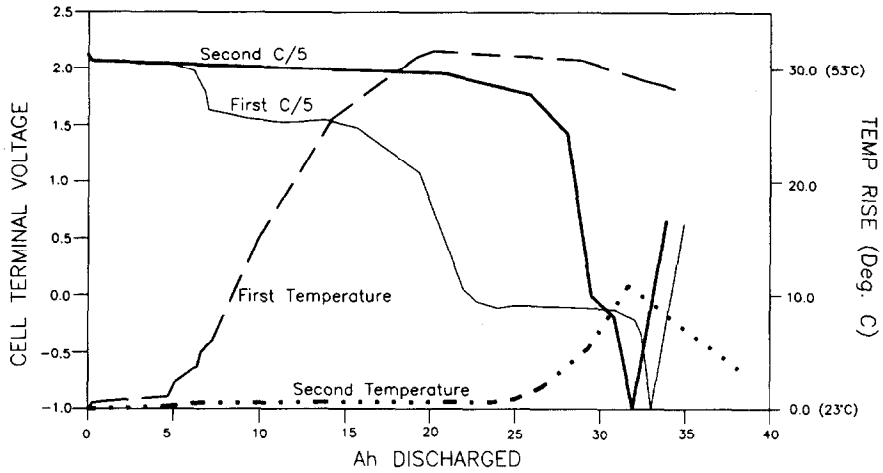

Fig. 6. 2 V/25 A h field return discharge data: thermal response: two $C/5$ discharges to -1.0 V, cell voltage and temperature.

correlates with the cell being driven past the primary discharge process, which is slightly endothermic. It appears that heat is generated in substantial quantities when the cell voltage drops to the secondary positive-plate discharge process. This may be due to PbO_2 discharge through the PbO/$PbSO_4$ passivation layer; the latter acts as a resistor on the positive grid and thus generates heat and depresses the discharge plateau by some amount proportional to its severity. In field applications, this could lead to battery failure due to temporary (1–10 h?) heat build-up that could easily soften plastic parts and thus possibly damage vent and/or terminal seals. For a large battery with poor heat dissipation properties, it is not inconceivable that 'meltdown' could occur during a long discharge with substantial i^2R heating. This is especially serious because it is unexpected; overheating should not occur during discharge! It is clearly dangerous to extrapolate from one experiment, but the fact that a skin temperature of 54 °C was attained for a small, cylindrical cell (high surface area for heat dissipation) on a low-rate discharge suggests that much higher temperatures could be realized by some batteries in certain applications.

The incorporation of tin into the positive grid, done primarily to afford recovery from deep discharge, has also been reported to enhance charge acceptance [30, 34] and improve cycling performance [31, 34]. Figure 7 shows cycle/capacity curves for a $C/5$, one cycle per day, regime through twenty cycles. It is apparent that the presence of tin in the positive grid has a dramatic effect on moderating the '20-cycle dip' phenomenon shown in Fig. 3 for cells and batteries using pure lead grids. At a 0.7 wt.% tin binary alloy level, it appears that the tin has a good short-term impact and helps batteries to maintain capacity during deep cycling to some extent, but not completely. Long-term cycle/capacity plots show some improvement over pure lead, but not to a significant degree.

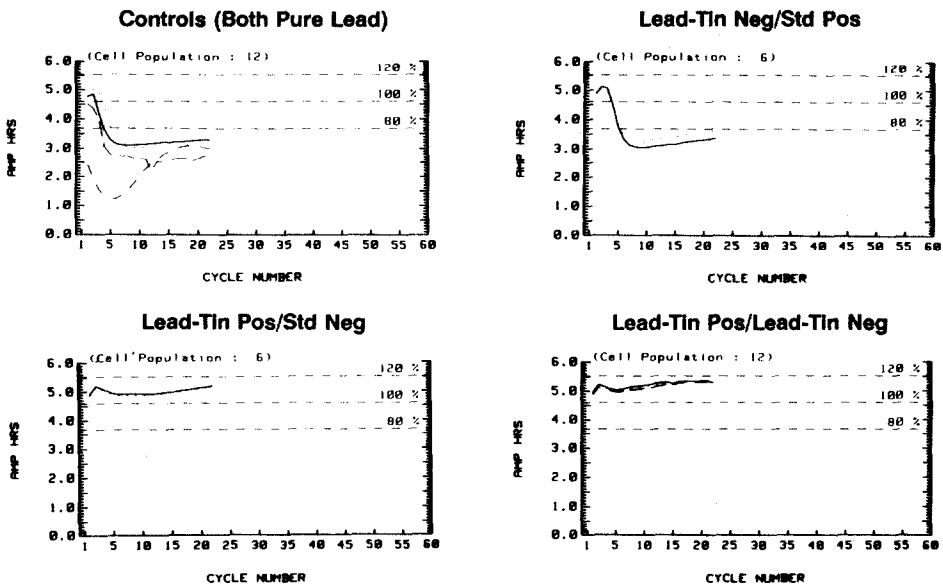

Fig. 7. Cycle/capacity plots for 6 V/5.0 A h batteries with various pure lead/lead–tin grid combinations.

Clearly, simple incorporation of low levels of tin into the positive plate is not sufficient to inhibit capacity loss to the extent desired, as shown in Fig. 8 for a 25 A h prismatic cell with lead–tin positive grids. This is a UPS system prototype unit that had been cycled on a 120 W constant-power discharge to 1.67 V with a 2.45 V constant-voltage recharge regime. The capacity gradually reduced to a discharge time of about 2 min at 250 cycles. At this point, the cell was given three $C/50$ discharges to -1.0 V with intermittent recharges, and then put back on cycling. After a further 27 cycles, the capacity reached the rated level and was slowly increasing. Monitoring of the cell and plate voltages through the three overdischarges showed double discharge plateaux for the cell; these changed through the discharges, but did not coalesce into one. As with pure lead cells, the negative voltage changed only slowly until the end of the discharge and the cell voltage excursions were due mainly to the positive.

In cycling applications, it appears that lead–tin cells/batteries will generally have much-improved early-life charge acceptance with no attendant loss of capacity. In long-term cycling, however, capacity losses similar to those seen for pure lead cells can be experienced. Happily, one or more overdischarges will largely regain this capacity loss, at least for some interval of additional cycles.

Float studies

Although it is not the focal point of this presentation, the influence of positive-grid corrosion and/or passivation in float applications is noteworthy.

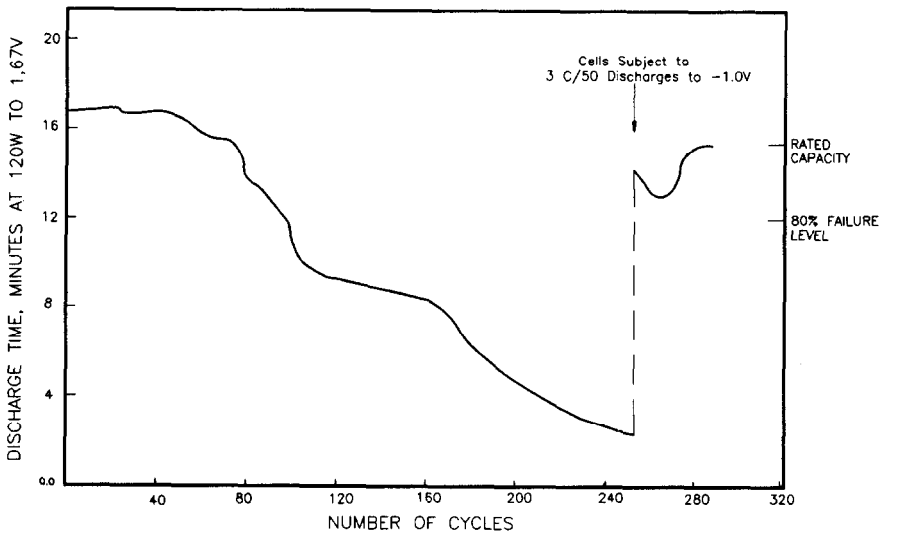

Fig. 8. Constant-power 120 W discharge capacity/cycle curves for 2 V/25 A h lead–tin grid cells.

In order to assess design lifetimes, accelerated-temperature float studies are often carried out to shorten failure times from years down to months or even weeks. In accelerated-float studies on pure lead cells and batteries carried out at 80 °C and 2.30 or 2.40 V/cell float voltages, it has been found that the predicted lifetimes of 55 or 37 days, respectively, were always met or exceeded, sometimes by a factor of two or three. Moreover, it was more likely that cells would fail due to top lead corrosion, with grid corrosion sometimes being minimial or non-existent. Similar experiments with cells/batteries with lead–tin positives had different outcomes; predicted lifetimes were achieved and exceeded by small amounts, but not nearly to the extent seen in pure lead cells. Moreover, cells failed due to positive grid corrosion in all cases, with the top lead being largely intact.

The unusually strong resistance of pure lead grids (but not top lead) to corrosion on float is apparently due to the protective nature of the passivation layer, as seen in Fig. 9. Samples were taken off 2.40 V/cell constant-voltage float at 80 °C after 18 and 40 days for examination. Samples were also investigated immediately after formation and at this stage a passivation layer had just begun to develop at the grid/active-material interface. After 18 days on float (Fig. 9(a)), a layer is clearly visible and little or no grid corrosion has occurred. At 40 days, the layer has grown to a thickness of about 20 μm (Fig. 9(b)) and, again, grid corrosion is not apparent. This interval corresponds to the design life of the battery on float, some 7–10 years, and at this time the battery still delivered more than 80% of its rated capacity. Autopsy indicated that the eventual failure would be due to corrosion of the top lead, which was substantial at this time.

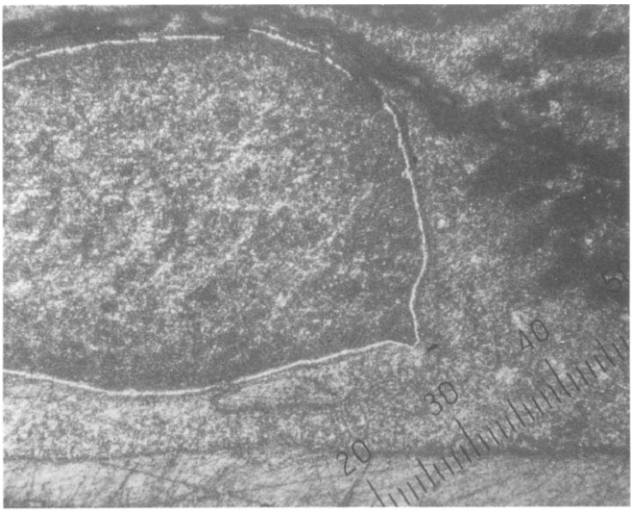

(a)

(b)

Fig. 9 Photomicrographs of pure lead positive grids from 12 V/55 A h batteries on float at 80 °C and 2.40 V/cell; 56 × magnification, each division = 25 μm: (a) 18 days, (b) 40 days (end of life).

Figure 10 shows similar data for batteries made with lead–0.65wt.% tin in the positive grids. It can be seen that corrosion has begun at 18 days; by 40 days it is substantial. Note in Fig. 10(a) that a passivation layer is present, and has about the same thickness as that formed on pure lead. Corrosion apparently occurs along the grain boundaries where the tin is slightly concentrated [34] and the grid alloy structure may be 'looser' and more susceptible to attack. The battery in Fig. 9(b) also had marginally acceptable discharge capacity, but experience with this test and others indicates that failure is imminent for lead–tin grid batteries at this point.

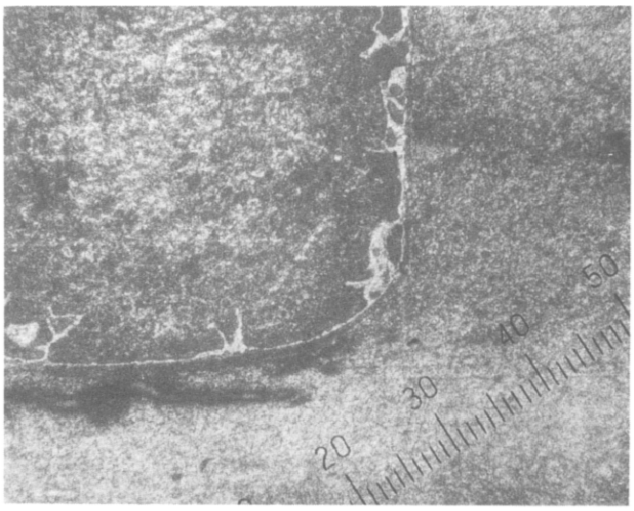

(a)

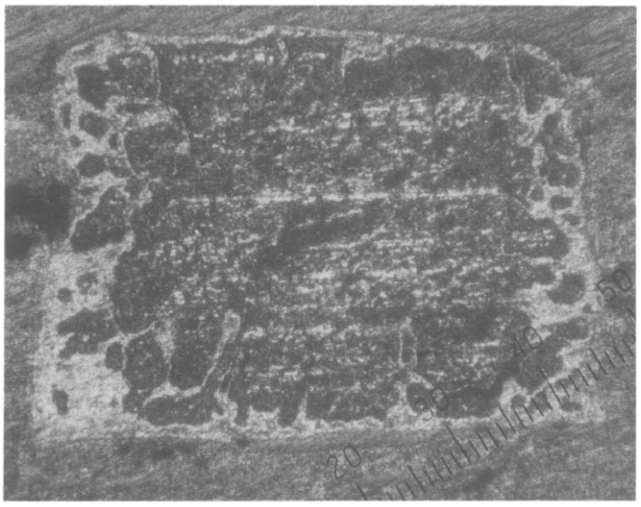

(b)

Fig. 10. Photomicrographs of lead–0.65wt.% tin positive grids from 12 V/55 A h batteries on float at 80 °C and 2.40 V/cell; 56 × magnification, each division = 25 μm: (a) 18 days, (b) 40 days (end of life).

The growth of the passivation layer on float and its protective nature with regard to anodic grid corrosion for pure lead are noteworthy. It is also significant that the same passivation layer forms on lead–tin grids (both on float and in cycling applications, even after formation), but not to the extent that corrosion is completely inhibited. The grain boundaries are still open to attack and as it turns out this is a mixed blessing. It should be noted that in accelerated testing of cells with pure lead grids that had passivated, such as in Fig. 9(b), acceptable capacities would still be delivered; the presence of the passivation layer does not necessarily produce battery failure on float.

Discussion

Pure lead

The formation of a $PbO_x/PbSO_4$ passivation layer on pure lead positive grids is well documented. The effects, however, in functional cells and batteries are not so well characterized.

From these studies and other work not published here, it appears that passivation of the positive grid can begin early in cell processing. If red lead is used in the positive paste and heat is available (for example, paste mixing, drying, filling, formation) thermopassivation can occur. It has been reported to take place in formed, dried plates or during open-circuit stand [35], but conceptually it can occur at other stages. The variability in the size of the passivation layer (Fig. 11) for pure lead grids made in two different locations using different materials and processing attests to this fact. A single product over time has also shown similar variances. At this point in time, it can only be safely said that both materials and processing can have a substantial impact upon the size of the passivation layer.

It is also clear from cycling and float data that the layer can grow and/or diminish during service. In float applications, it clearly grows with time and as this occurs the decrease in discharge capacity becomes more severe. In cycling, it can lead to rapid capacity loss or, if less prominent, to an 'early-cycle dip' and subsequent recovery of capacity. If the battery or cell crashes, as shown in Fig. 3, curve C, it is probable that there is a progressive build-up of lead sulphate and PbO_x near the grid surface to the point where charge acceptance is so low that the unit 'steps down' during successive cycles. When a dip and recovery is seen, it may be that the electrolyte distribution is such that sulphate deposition in the plates reduces the electrolyte specific gravity to the point where the lead sulphate solubility increases and/or cracks may develop, allowing electrolyte to penetrate through the perm-selective membrane layer. This hypothesis is supported by the fact that a reduction in electrolyte specific gravity from 1.350 to 1.280 in cells that are otherwise identical results in a dramatic 'flattening out' of the cycle/capacity curve to a point where no dip can be seen [36] and performance is consistently like that shown in Fig. 3, curve A, but with diminished nominal capacity. Studies now in process should help to clarify this important but largely speculative point.

Once formed, the passivation layer is not permanent. In most cases, however, methods for overcoming the effect of the layer are not practical in field applications. Passivation of the positive grid is minimized or eliminated in the following ways:

- storage at ambient temperatures for several months
- a 'heat soak' at temperatures of 50 to 60 °C for several weeks
- deep discharge or overdischarge below a cell voltage of ~1.3 V.

The first two approaches are basically the same, utilizing time and temperature to allow the lead sulphate barrier layer to digest and develop cracks to allow acid penetration to the grid surface. The third approach probably

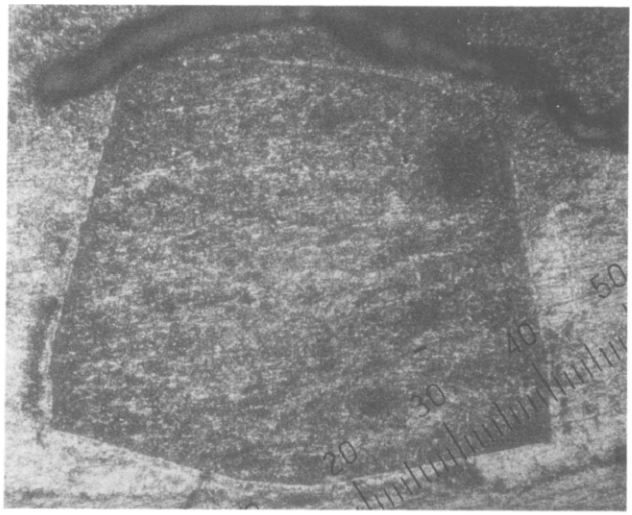

(a)

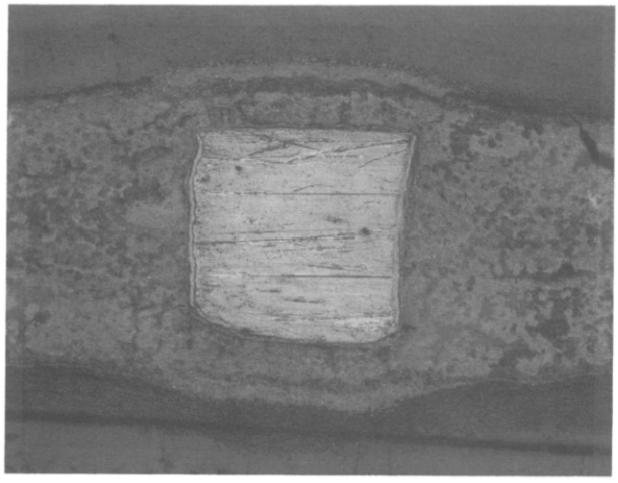

(b)

Fig. 11. Photomicrographs of pure lead positive grid members off formation: (a) 12 V/55 A h automotive battery produced in Denver, 56 × magnification; (b) 2 V/5 A h cell produced in Warrensburg, 35 × magnification.

involves electrochemical consumption of the $PbO_x/PbSO_4$ layer(s), although this has not been proven. According to the E'_0 values in Table 1, a cell voltage of about 0.6 V, or lower, should be necessary to convert PbO or $PbSO_4$ to lead metal on the positive, but it has been empirically observed that considerably higher cut-off voltages will lengthen the primary discharge plateau on subsequent cycles. Clearly, this process is not completely characterized.

Cells with moderate levels of passivation display a double discharge plateau, such as that seen in Fig. 6. It is speculated that this is a further

discharge of β-PbO_2 beyond the primary plateau, but lowered due to the resistive nature of the passivation layer. When the latter is severe, only a single normal plateau is seen and apparently the resistance is so great that any further discharge has to occur below the positive-plate background voltage for $PbSO_4/Pb$ conversion, about -1.0 V versus Hg/Hg_2SO_4.

At the normal cut-off voltages for deep-cycling applications, 1.6 to 1.9 V, cells with pure lead positive grids will also suffer from some degree of passivation as the latter builds up during overcharge. In extreme cases, this results in early-cycle failure (Fig. 3, curve C) or '20 cycle dip' and recovery (Fig. 3, curve B). It has been our experience that once a battery has been through this 'dip', the recovery is complete and the expected cycle-life is quite large. Failure after 200 to 300 deep cycles has not been extensively investigated for pure lead cells, but it is not felt that it is due to the passivation phenomenon; rather, is more likely related to degradation of the positive active material morphology.

Lead–tin

Careful inspection of the literature verifies that tin alloyed into the positive grid and/or applied as a surface layer is initially helpful in facilitating recovery from deep discharge but such influence in short- and long-term deep-cycling applications is less certain. Moreover, there is considerable diversity in the views of the mechanism of tin action, ranging from a simple redox process between PbO and SnO [24] to complex semiconductor processes [21, 35]. An open question, though, is the fate of the tin and its effectiveness in different valence states. Tin is relatively easily oxidized and, in the environment of the positive plate, will be converted to Sn(IV). SnO_2 is very stable in the positive plate [37] and is resistant to conversion back to lower oxidation states except upon electrode reversal. Thus, any mechanism requiring the presence of Sn(II) will be germane only as long as this species is available. It has been reported that a 5 μm grid coating of tin metal is completely oxidized and dispersed into the surrounding active material even just after formation and has no beneficial effect on cycle-life in this form [38]. The lack of a positive effect of tin upon life in deep-cycling applications has been verified recently [26] and so some question remains as to what its influence may be, long term, in cycling duties.

The grids involved in this study were lead–0.6 to 0.7 wt.% tin binary alloys. In deep-discharge, cycling and float studies, it appears that a different mechanism from those previously reported is operative. Figure 12 demonstrates that lead–tin grid cells clearly have a passivation layer even following formation. It is of variable thickness but looks to be continuous. Thus, it seems that the presence of tin in chill-cast sheet at the 0.6 to 0.7 wt.% level does not prevent the formation of a passivation layer. Upon closer inspection, however, using SEM/EDAX for tin, lead and sulphur mapping, it can be seen that on pure lead the layer is, indeed, continuous. On lead–tin, by contrast, there are small corrosion sites here and there on the grid surface. These are filled with lead sulphate but they are also slightly enriched in tin and

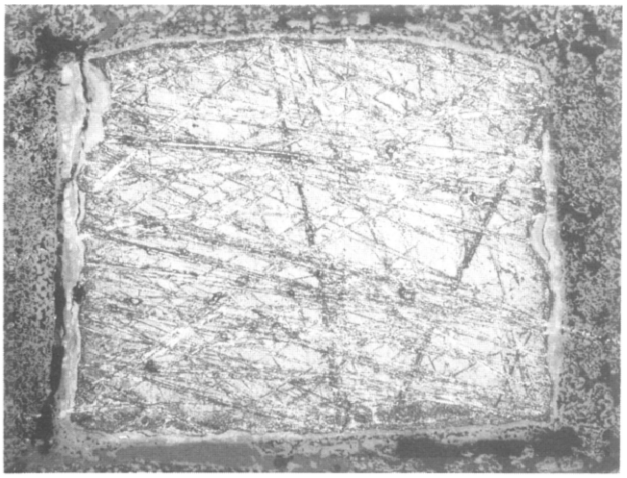

(a)

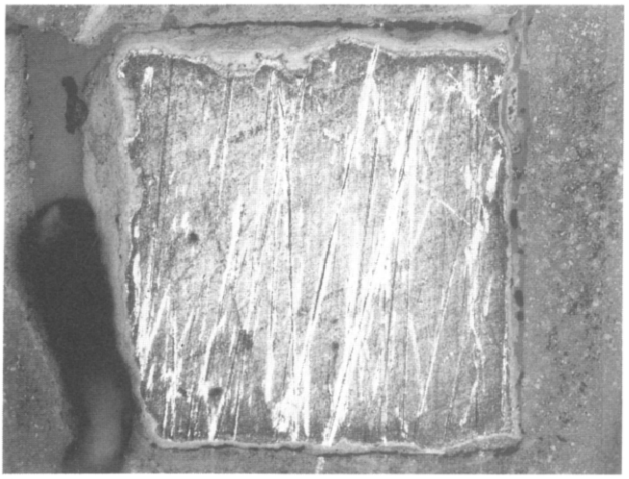

(b)

Fig. 12. Photomicrographs of pure lead (a) and lead–tin (b) positive grid members off formation; 70 × magnification: (a) pure lead, (b) lead–0.7% tin.

apparently do not allow the passivation layer to form. Tin enrichment and subsequent corrosive attack along grain boundaries is documented for lead–tin alloys [39] and the progression of this is obvious in Fig. 10. The slight enrichment in the grain boundaries may help to keep these areas open, but overall the tin remains homogeneously distributed in grids made by chill-cast or cold-rolled processes where tin migration is minimal.

Thus, while much of the lead–tin grid surface is passivated, apparently in the same way and form as with pure lead, corrosion sites at grain boundaries and perhaps within some grain bodies remain open and allow unimpeded current flow to some extent. It is obvious from this observation

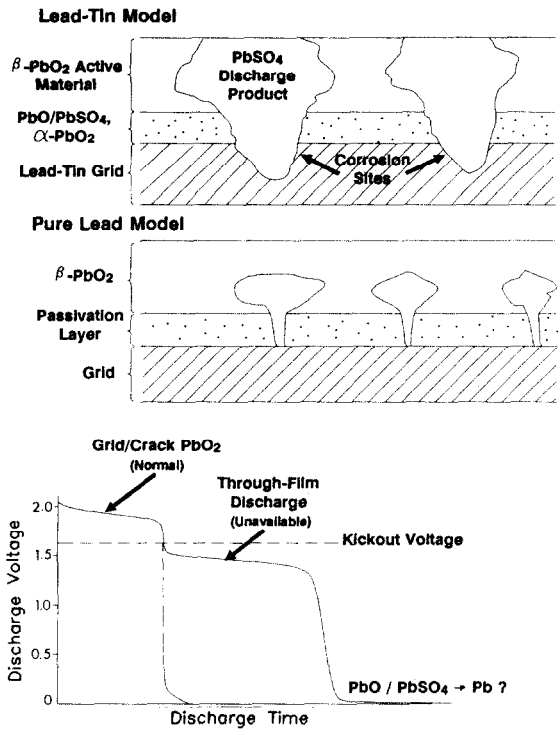

Fig. 13. Conceptual view of positive plate discharges in the presence of a passivation layer.

that the nominal tin level, the alloy composition and the grid preparation conditions may all be critical in providing the positive grid with optimal protection from passivation. The mixed blessing may be, however, that good passivation protection may also entail shortened life due to accelerated grid corrosion. It readily follows that different grid structures may be optimal for float and deep-cycling applications.

Figure 13 shows a conceptual model for what may be taking place at pure lead and lead–tin positive grid/active-material interfaces during discharge or overdischarge, based upon the data presented herein. At low discharge rates, the primary discharge plateau is at about 2.0 V and is of variable duration. If the passivation effect is severe, the cell voltage drops to about zero volts directly and stays at that level until the negative plate capacity is exhausted (dotted line).

With a normal kickout voltage of about 1.7 V, this cell would be deemed to have very low capacity. The material being discharged during this step is either PbO_2 at the grid surface or material accessible through cracks or gaps in the membrane layer; for the lead–tin model it would be PbO_2 discharged at and around the corrosion sites.

At the end of the first discharge step, access to additional PbO_2 has been choked off by the $PbSO_4$ 'blossoms' formed from the grid surface. If the

resistance of this $PbSO_4$ and the passivation layer is sufficiently low a second plateau will be seen, usually below the normal cut-off voltage, and thus for all practical purposes unavailable. The sum of the two plateaux in terms of discharge time can, however, represent the majority of the capacity normally available.

When the cell voltage drops to near zero volts, the negative plate will have a potential of about -0.1 V versus Hg/Hg_2SO_4 and the positive will have been driven to about the same value. Any PbO or $PbSO_4$ at the grid surface should be reduced and thus the passivation layer should be damaged or destroyed; subsequent discharges should show a much-enhanced initial plateau and a corresponding change in any follow-up steps. It has been our experience that one or more of these deep discharges will restore a cell's capacity to its rated level, but how long this lasts has still not been defined.

Clearly, this phenomonen bears some similarity to the nickel–cadmium 'memory effect' in the shape of the discharge curve and the method of remedy. At this point it is specific for pure lead and it may, or may not, apply to lead–calcium positive grids.

Conclusions

Pure lead grids are noteworthy in float and cycling applications due to the inherent corrosion resistance of lead metal. The grid/active-material interface can, however, experience formation of a passivating layer that protects the grid from corrosion, but results in diminished charge acceptance, leading in some cases to moderate to rapid loss of discharge capacity in both float and deep-cycling applications. The passivation can be reversed by allowing time and temperature to dissolve some of the layer or by one or more deep discharges. In most field applications, however, this is not feasible.

The incorporation of tin into the positive grid has long been known to improve charge acceptance and afford the ability to easily recover batteries from deep discharge or overdischarge. Various mechanisms have been proposed for this 'tin effect', ranging from the simple redox reaction $SnO + PbO \rightleftharpoons Pb + SnO_2$ to a semiconductor-type doping of PbO_x with tin. This study has demonstrated that an alternate process may take place in functional VRLA batteries. Consequently, formation of the passivating $PbO_x/PbSO_4$ layer is at least initially inhibited both at grain boundary sites on the grid surface, and possibly later within some grain bodies where corrosion is enhanced and these areas thus remain open for current flow. As it turns out this is a mixed blessing, for although the presence of more corrosion sites will minimize the effect of the passivation layer, it may also shorten life as the grid degrades more readily.

Nevertheless, charge acceptance is improved and early-life cycle/capacity dip or crash is greatly ameliorated. Long-term cycle-life may also be extended due to the improved overall charge acceptance and delivery, but this has not been demonstrated. While charge acceptance is improved by

using lead–0.6 to 0.7 wt.% tin binary alloys, more work needs to be carried out to optimize the benefits that may be realized from full utilization of the 'tin effect' in deep-cycling applications. Right now, it is more likely that the major contribution of tin is getting the battery safely through the first 20–30 cycles.

Acknowledgements

Thanks are due to La Donna Martin for preparation of the manuscript and to Mary Sahs for the graphics work. Much of the experimental work was carried out by David Wisdom, Brian Longenecker, Bob Stosky and Cathy Shadburn and this is gratefully acknowledged. Discussions with Michael Kepros were also of great value. Presentation of this work at the Second European Battery Conference was jointly sponsored by Gates Energy Products and Portable Energy Products.

References

1 E. F. Wolf and C. F. Bonilla, *Trans. Electrochem. Soc.*, *79* (1941) 307.
2 J. J. Lander, *J. Electrochem. Soc.*, *98* (1951) 213.
3 J. J. Lander, *J. Electrochem. Soc.*, *98* (1951) 220.
4 J. Burbank, *J. Electrochem. Soc.*, *106* (1959) 369; *103* (1956) 87.
5 J. J. Lander, *J. Electrochem. Soc.*, *103* (1956) 1.
6 P. Rüetschi, *J. Electrochem. Soc.*, *120* (1973) 331, and refs. therein.
7 D. Pavlov, *Ber. Bunsenges. Phys. Chem.*, *71* (1967) 398.
8 D. Pavlov, *Electrochim. Acta*, *13* (1968) 2051.
9 D. Pavlov, C. N. Poulieff, E. Klaja and N. Iordanov, *J. Electrochem. Soc.*, *116* (1969) 316.
10 D. Pavlov and R. Popova, *Electrochim. Acta*, *15* (1970) 1483.
11 D. Pavlov and N. Iordanov, *J. Electrochem. Soc.*, *117* (1970) 1103.
12 K. R. Bullock and E. C. Laird, *J. Electrochem. Soc.*, *129* (1982) 1393.
13 K. R. Bullock and M. A. Butler, *J. Electrochem. Soc.*, *133* (1986) 1085.
14 S. Tudor, A. Weisstuch and S. H. Davang, *Electrochem. Technol.*, *3* (1965) 90.
15 S. Tudor, A. Weisstuch and S. H. Davang, *Electrochem. Technol.*, *4* (1966) 406.
16 S. Tudor, A. Weisstuch and S. H. Davang, *Electrochem. Technol.*, *5* (1967) 21.
17 D. Pavlov and S. Ruevski, *J. Electrochem. Soc.*, *126* (1979) 1100.
18 K. Wiesner, J. Garche and N. Anastasijević, in J. Thompson (ed.), *Power Sources 9*, Academic Press, London, 1983, p. 17, and refs. therein.
19 J. Perkins and G. R. Edwards, *J. Mater. Sci.*, *10* (1975) 136, and refs. therein.
20 J. Perkins, *Mater. Sci. Eng.*, *28* (1977) 167, and refs. therein.
21 D. Pavlov, B. Monakhov, M. Maja and N. Penazzi, *J. Electrochem. Soc.*, *136* (1989) 27.
22 Z. Takehara, K. Kanamura and M. Kawanami, *J. Electrochem. Soc.*, *137* (1990) 800.
23 Z. Takehara, K. Kanamura and M. Kawanami, *J. Electrochem. Soc.*, *136* (1989) 620.
24 M. Terada, S. Saito, T. Hayakawa and A. Komaki, *Prog. Batt. Solar Cells*, *8* (1989) 214.
25 H. Yasuda, S. Furuya, N. Hoshihara, T. Yamaguchi, K. Takahashi and T. Ishii, *U.S. Patent 4 805 277* (1989).
26 S. Saito, M. Terada, T. Hayakawa, A. Miura and A. Komaki, *U.K. Patent GB 2 209 241-A* (1989).
27 W. F. K. Wynne-Jones, W. H. Beck and R. J. Doran, *U.K. Patent 651 614* (1951).

28 K.-H. Christian, H. Döring, J. Garche, K. Wiesener and G. Schadlich, *E. Ger. Patent DD 257 144 A1* (1988).
29 H. Döring, J. Garche, W. Fischer and K. Wiesener, *J. Power Sources, 28* (1989) 367.
30 H. K. Giess, in K. R. Bullock and D. Pavlov (eds.), *Advances in Lead–Acid Batteries*, The Electrochemical Society Softbound Series PV 84-14, Pennington, NJ, 1984, p. 241.
31 K. Wiesener, J. Garche and N. Anastasijevíc, in J. Thompson (ed.) *Power Sources 9*, Academic Press, London, 1983, p. 36.
32 J. J. Lander, *J. Electrochem. Soc., 99* (1952) 467.
33 A. G. Cannone, *U.S. Patent 4 605 605* (1986).
34 D. Wisdom and R. F. Nelson, Paper presented at *10th Int. Lead Conf. Pb90, Nice, France, May 1990.*
35 H. Döring, J. Garche, H. Dietz and K. Wiesener, *J. Power Sources, 30* (1990) 41.
36 R. F. Nelson, unpublished data.
37 J. J. Rowlette, S. A. Alkaitis, N. Pinsky and J. Y. Josefowicz, *21st Int. Energy Conversion Engineering Conf., San Diego, CA, Aug. 25–29, 1986*, pp. 1052–1056.
38 K. Fuchida, K. Okada, S. Hattori, M. Kono, T. Takayama and Y. Nakayama, *ILZRO Rep. No. LE-276, Prog. Rep. No. 7*, Yuasa Battery Co., 1981.
39 J. L. Dawson, in A. T. Kuhn (ed.), *The Electrochemistry of Lead*, Academic Press, London, 1979, p. 342, and refs. therein.